UDC 539.375.5 : 620.186.4
669.384.019

Branching in Distributed Cracks

分布き裂の分岐

Yoshiaki HAGIUDA* and Masahisa MATSUNAGA*

萩生田善明・松永正久

1. Introduction

In a previous report [1], the present authors discussed natures of the uniformly distributed cracks grown on electrodeposited bright copper on ABS plastics, and found that the number of distributed cracks and the propagating rates were saturated after the stress repetition of 70 per cent of the fatigue life. At nearly the same period, the length of the cracks also saturated and the final length was of the same order of thickness of the deposits. When the growth of the cracks was stopped, branching occurred, especially in the case of cracks in torsion fatigue. This branching phenomenon corresponded to one of the appearances of transition from stage I to stage II in fracture process.

In measuring many branching angles, it was found that the linear fracture mechanics were applicable in assuming the homogeneous unifom body in a case of small crystal, and that the crystallographic behaviors predominated in the case of more coarse crystal. When the branching did not occur, the cracks were crossed or embodied with each other.

2. Methods of Experiments

Specimens of elctrodeposited copper were shown in the previous report [2] and classified A and B which had grain size of 0.2 to 0.3 μm and about 1 μm, respectively. Photographs of the surfaces are shown in Fig. 1. Experiments were perfomed by repeated torsion, and strain amplitude was $\gamma_a=(0.9 \text{ to } 1.5)\times 10^{-3}$, number of repetition was $N=10^{-5}$ to 10^{-6}

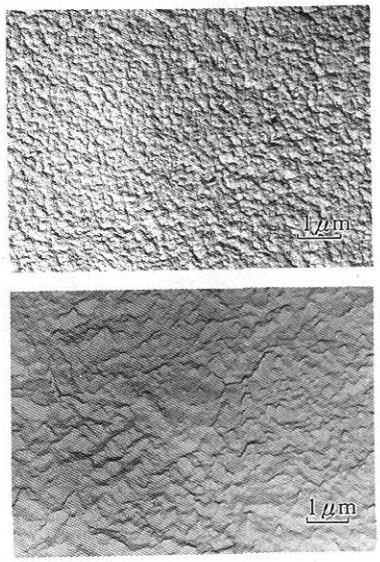

Fig. 1 Crystal structure of electrodeposited copper (a) Specimen A, grain size: 0.2 to 0.3 μm. (b) Specimen B, grain size : about 1 μm

3. Experimental Results

3.1 Branching in the distributed cracks

The mode of branching was affected by grain size of deposits, mode of repeated stress and thickness of deposits etc. In this experiments, angle and shape of

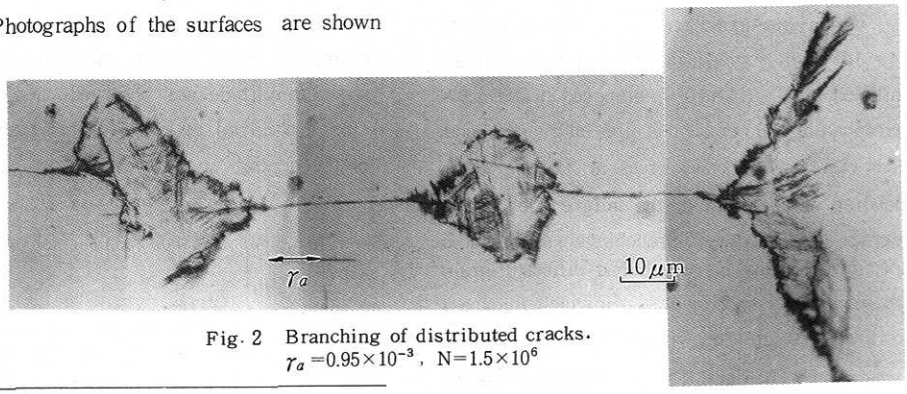

Fig. 2 Branching of distributed cracks. $\gamma_a=0.95\times10^{-3}$, $N=1.5\times10^{6}$

* Dept. of Mechanical Engineering and Naval Architecture, Institute of Industrial Science, Univ. of Tokyo

branching, formation of subsidiary cracks, and interaction or crossing with other cracks were observed. Fig. 2 shows an appearance of many cracks lying linearly along the direction of maximum shearing stress and crossing each other after growth and branching, when the specimen was broken at $N = 1.5 \times 10^{-6}$ with $\gamma_a = 0.95 \times 10^{-3}$.

These branchings was frequently accompanied by cracks furthermore branched or propagated along the direction of shearing stress, as shown at the left-hand side and right-hand side of the figure, respectively. A central part of the figure indicates the coincidence of cracks curved after branching. Fig.3. shows an

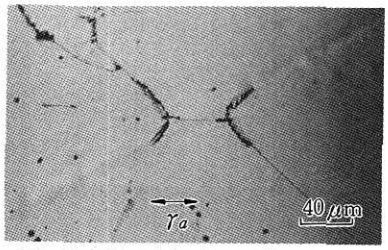

Fig. 3 Transition from distribued cracks to stage II cracks

example in which stage II cracks were originated from the branched cracks. In this case, the branching and stage II crack were distinguished clearly, and the branching could be estimated as a kind of transition effect. However, the process was not always uniform, and affected by grain size of deposits as shown in the following section.

3.2 Maximum crack length without branching

The maximum length of cracks propagated linearly without branching was not predicted. An example of the process from initiation to branching is shown in Fig. 4., which was found on a specimen broken at $N = 3.4 \times 10^5$ with $\gamma_a = 1.09 \times 10^{-3}$. Two linear cracks were initiated at $N = 1.4 \times 10^5$, branched at $N = 1.8 \times 10^5$ corresponding 50 per cent of the fatigue life and coincided with a neighboring crack at $N = 2.52 \times 10^5$, corresponding 70 per cent of the fatigue life.

The crack length between branchings was measured with specimens A and B, which had different grain size. A result in a specimen A, in which thickness of deposit was 29 μm, $\gamma_a = 0.95 \times 10^{-3}$ and $N = 1.5 \times 10^6$, was shown in Fig. 5. The distribution of length was fairly wide. Most frequent values were 40 to 50 μm and mean value 53.8 μm. Another result in a

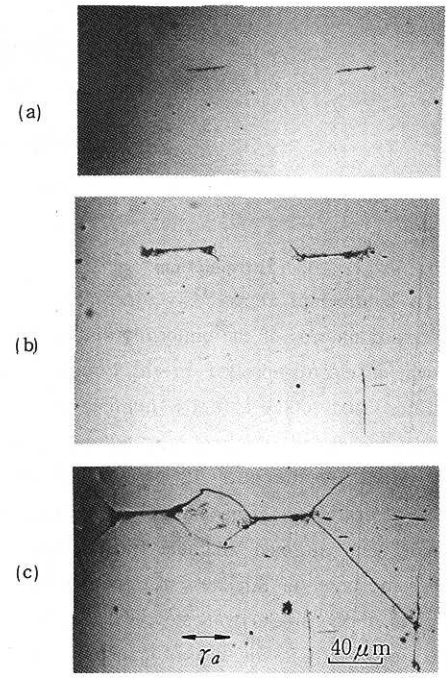

Fig. 4 Process from initiation of cracks to branching (a) $n = 1.4 \times 10^5$, (b) $n = 1.8 \times 10^5$, (c) $n = 2.4 \times 10^5$, $\gamma_a = 1.09 \times 10^{-3}$, $N = 3.4 \times 10^5$

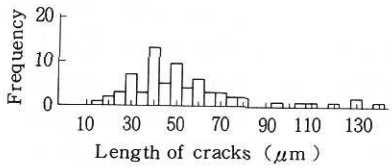

Fig. 5 Distribution of the maximum crack length between branching. (Specimen A, number of measurments n=70, mean value $\bar{x} = 53.8$ μm, standard deviation s=26.6 μm)

specimen B, in which the thickness of deposit was 35 μm, $\gamma_a = 1.2 \times 10^{-3}$ and $N = 1.15 \times 10^5$, was shown in Fig. 6. The mean length was 49.3 μm. In comparing these lengths, no effect on grain size and stress amplitude was observed, and nearly all branchings occurred at longer length than the thickness of the deposit.

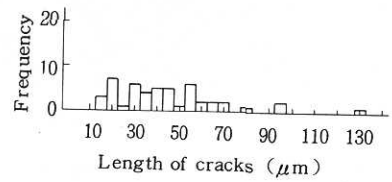

Fig. 6 The same (Specimen B, n=49, $\bar{x} = 49.3$ μm), s =42.1 μm)

3.3 Application of linear fracture mechanics on branching angle

It was assumed in the previous report[2], that the maximum length of cracks was nearly coincided with the thickness of the deposit, because the cracks propagated along the surface as well as to the interior, and branching occurred when these reached at the interface of the deposit and plastics, changing the stress condition at the advancing point of the crack. It was also assumed that the linear fracture mechanics were applicable at the branching point in considering the small crystal size of the deposit and low ductility.

In applying a fundamental equation, the stress components are expressed by equation (1)

$$\left.\begin{aligned}\sigma_x &= -\frac{K_{II}}{\sqrt{2\pi r}} \sin\frac{\theta}{2}\left\{2+\cos\frac{\theta}{2}\cos\frac{3\theta}{2}\right\}\\ \sigma_y &= \frac{K_{II}}{\sqrt{2\pi r}} \sin\frac{\theta}{2}\cos\frac{\theta}{2}\cos\frac{3\theta}{2}\\ \tau_{xy} &= \frac{K_{II}}{\sqrt{2\pi r}} \cos\frac{\theta}{2}\left\{1-\sin\frac{\theta}{2}\sin\frac{3\theta}{2}\right\}\end{aligned}\right\} \quad (1)$$

if the stress distribution near the fracture in shearing stress field is expreseed as shown in Fig. 7.

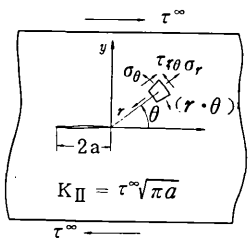

Fig. 7 Stress components at advancing edge of a crack in the case of torsion test

If $(\sigma_x, \sigma_y, \tau_{xy})$ are tranformed by $(\sigma_r, \sigma_\theta, \sigma_{r\theta})$, the following equations (2) could be obtained.

$$\left.\begin{aligned}\sigma_r &= \sigma_x\cos^2\theta+\sigma_y\sin^2\theta+\tau_{xy}\sin 2\theta\\ \sigma_\theta &= \sigma_x\sin^2\theta+\sigma_y\cos^2\theta-\tau_{xy}\sin 2\theta\\ \tau_{r\theta} &= \frac{\sigma_y-\sigma_x}{2}\sin 2\theta+\tau_{xy}\sin 2\theta\end{aligned}\right\} \quad (2)$$

A result of numerical calculations of such stress component as a function of θ is shown in Fig. 8. in putting

$$\frac{K_{II}}{\sqrt{2\pi r}} = \tau^\infty\sqrt{\frac{a}{2r}} \equiv 1$$

It was found that each component was symmetrical with $\theta=0$, that σ_θ had its maximum value at $\theta=\pm 71°$, that $\tau_{r\theta}$ had its maximum value at $\theta=0°$, and that σ_r was relatively small. It was assumed that σ_θ must predominate in referring the mode of branching described in the preceding section, but that $\tau_{r\theta}$ also affected the propagation of cracks. This caused the subsidary cracks along $\theta=0°$ and minute cracks propagated from the branched cracks even after branching.

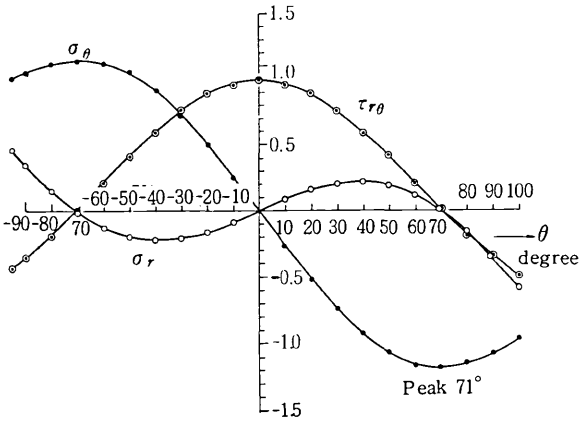

Fig. 8 Variation of stress components near a crack tip in the case of torsion test

3.4 Statistic values of branching angle

Effect of thickness of deposits on branching angles was investigated. Experiments were performed with specimens A and B, mentioned in the previous section. In these specimens, cracks propagated mainly in two branches. Angles between these at the branching points and mean angles including propagated ones were measured. The former is called "initial angle" and the other is called "mean angle" in this report.

Fig. 9. shows the distribution of 183 initial angles on the specimen A which had minute grain

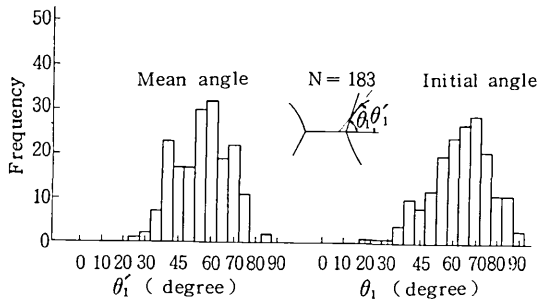

Fig. 9 Distribution of branching angles, specimen A and minute grain size.

研 究 速 報

size. It was found that the most frequent value of the initial angles was 70°, mean value 63.2°, standard deviation 13.7°. It was also found that the most frequent value of the mean angles was 60°, mean value 49°, and standard deviation 13.7°. It was concluded from these results that the initial angles coincided approximately with the direction of maximum σ_θ calculated by the theory.

The values of mean angles indicated gradual change of direction in crack propagation. Some of these cracks propagated along the direction of 45°. About 20 per cent of cracks had their subsidiary ones extended along the direction of the shearing stress, that is, $\theta=0°$.

Fig. 10. shows the branched cracks appeared on the specimen B which had a little larger grain size.

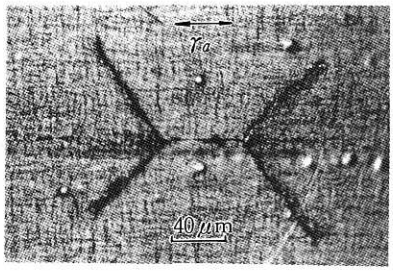

Fig. 10. Branching in specimen B which had a little larger grain size. It is shown that the branching angle is 45°. $\gamma_a=1.2\times10^{-3}$, N=1.15×105

In this case, the branched cracks propagated along the direction of stage II cracks at the branching point. The minute slips on the surface exhibited the crystallogrophic behavior. Fig. 11. shows the distribution of 239 initial and mean angles. The most frequent value of the initial angle was 45°, mean value 43.9°, and standard deviation 16.7°. In the mean angles, the most frequent value was 50°, mean value 45.8°, and standard deviation 12.3°. It was shown that the grain size had effect on the mode of branching, but finally the cracks propagated as stage II ones. It was hypothesized that branching occurred when the distributed cracks attained the interface of the deposit and plastics.

Shorter cracks than the thickness of the deposit would originate from a defect as shown in Fig. 12, or from unbalancing of propagation to the depth direction In repeated bending, few branching occurred. They crossed frequently with other ones and transition to stage II cracks from the advancing point

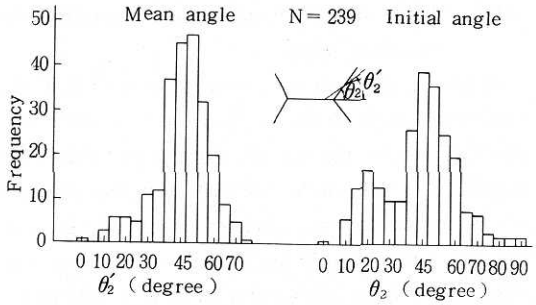

Fig. 11. Distribution of branching angles, specimen B

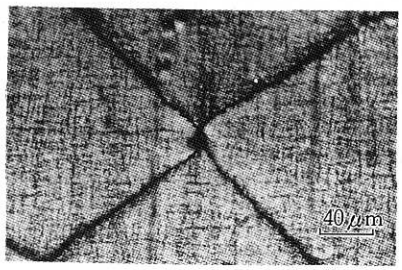

Fig. 12. Example of short cracks, originated from a defect and propagated as stage II crack

was not observed, since the difference among σ_θ, σ_r and $\tau_{r\theta}$ was smaller, as shown in Fig. 13.

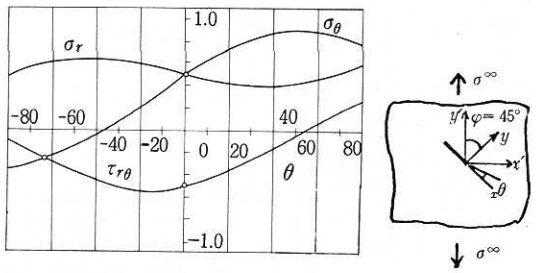

Fig. 13. Stress conponents in plane bending

Acknowledgements

The authors would like to express their thanks to Prof. H. Miyamoto, Dr. N. Chiba and Prof. H. Kitagawa for their encouragement and kind discussions. (Manuscript received, July 6, 1977)

References

1) M. Matsunaga and Y. Hagiuda, Fatigue Damage on Electroplated ABS Plastics, Proc of 8th INTER-FINISH, Forster-Verlag AG, Zürich. p. 377-382
2) Y. Hagiuda and M. Matsunaga, Jour. of Inst. Ind. Sci., Tokyo Univ. (Seisan Kenkyu) 29, 6, 327, 1977